

# Research on the Deposition Mechanisms and Production Characteristics of Untabulated Reservoirs in the X Oilfield of the Songliao Basin

Pan Wu

No.4 Oil Production Plant of Daqing Oilfield Company Ltd., Daqing 163511, China

**Abstract.** In the late stage of the ultra-high water cut development, the untabulated reservoir (not included in the submitted reserve sheet) is considered an important part of production sustainability in the X oilfield. According to the coring well data of 5 wells in the eastern district, the untabulated reservoir is associated with higher heterogeneity. Specifically, it develops not only the conventional low and ultra-low permeability sands but also medium-high permeability sands with thickness below 0.2 m. Given this, the research investigates the sedimentary models, spatial distribution, and heterogeneity of the different types of untabulated sand bodies, based on the core analysis. Moreover, the physical model water flooding experiments are carried out and the production characteristics of the different sand bodies in the untabulated reservoir with the different recovery approaches are clarified. The findings of this research effectively solve the development contradictions of the untabulated reservoir and lay down the foundation for the further potential tapping of the untabulated reservoir.

**Keywords:** Untabulated reservoir, sedimentary model, planar distribution, heterogeneity, recovery situation.

## 1. Introduction

Reservoir rocks of the Songliao Basin are derived from sediments of the fluvial-delta system of the intra-continental shallow-water lacustrine basin. The prolonged complex deposition is associated with not only sediments of high-energy environments but also those of low-energy environments with an insufficient supply of clasts. Such sediments of low-energy environments are mainly muddy siltstone characterized by the presented hydrocarbon occurrence of the oil patch and oil immersion, and located in the top, bottom, surrounding, and inside of the high-energy sediments. The corresponding reservoir rocks present degraded physical properties and are typically excluded from the effective reservoir rock. Therefore, they are not included in the reserve sheet and are referred to as the untabulated reservoir [1].

The X oilfield lies in the southern Songliao Basin and is associated extensive development of untabulated reservoirs. One drilled well encounters 48.6 independent untabulated sands on an average basis, with the sand thickness of 28.3 m, and the reserves of the untabulated reservoirs account for 17.9% of the total oil initially in place of the region. In 2015, five sealed-coring wells are placed in the eastern X oilfield, within 1000 m perpendicular to the provenance. The core samples reveal that the average permeability of the untabulated sands is  $12.5 \times 10^{-3} \mu\text{m}^2$  and the average porosity is 20%. Further

classification by permeability shows that the untabulated reservoirs are associated with an expanded range of air permeability. The maximum air permeability of the samples reaches  $1300 \times 10^{-3} \mu\text{m}^2$ , representing the high-permeability sandstone, while the lowest permeability is less than  $10 \times 10^{-3} \mu\text{m}^2$ , representing the ultra-low permeability sandstone.

Upon the arrival of the ultra-high water cut stage, the thin poor reservoirs, dominated by the untabulated reservoirs, have become the main target for water flooding-based reserve potential tapping in the X oilfield. As the low-efficient and insufficient circulation problems of injected water intensify, the development contradiction of the untabulated reservoirs becomes increasingly prominent. Given these, this research investigates the heterogeneity of the untabulated reservoirs, based on the samples of the five coring wells, in an attempt to clarify the sedimentary model and planar distribution of sand bodies with varying levels of permeability in the untabulated reservoirs. Moreover, the physical model flooding is carried out to reveal the production characteristics of untabulated reservoirs. Efforts of this research are made to further provide theoretical and practical references for the potential tapping of untabulated reservoirs.

## 2. Heterogeneity of untabulated reservoirs

### 2.1 Core characteristics of untabulated reservoirs

Two types of sandstone are identified in the untabulated reservoirs, according to the core characteristics of the coring wells. One is the low and ultra-low permeability sandstone, with permeability below  $50 \times 10^{-3} \mu\text{m}^2$ , which are classified as the conventional untabulated reservoir. It is seen with a predominance of muddy siltstone or silty mudstone, and diverse oil-containing attributes, mostly of oil patch and oil stain. Moreover, it features numerous inclusions of muddy strips or aggregates, and can be subdivided into three groups, namely strip-like, thin-bedded, and patchy. The other is the untabulated sand with permeability above  $50 \times 10^{-3} \mu\text{m}^2$  and called the favorable band. Its top and bottom contact with the low and ultra-low permeability stands, and the lithology is siltstone or fine sandstone. The oil-containing attribute is typically identified as oil immersion, with that of some samples reaching the oil-rich level. The oil occurrence of this type is more similar to that of the effective sandstone reservoir, and yet the corresponding thickness is less than 0.2 m, which results in failure of identification in well logs and subsequent inclusion into untabulated reservoirs (Fig. 1). Among the 522 untabulated samples in total collected from the Sa-Pu oil layers of the five coring wells, the conventional untabulated samples account for 44.8% of the total, constituting the main permeability range. However, the sand samples of the favorable bands also hold the shares of 29.4% (Table 1), which indicates that the interior of the untabulated reservoirs is associated with high intra-layer heterogeneity, due to the extensive development of favorable bands.

The water washing observation of the coring wells demonstrates that the development of favorable bands does not only affects the intra-layer heterogeneity of the untabulated reservoirs but also the production of these reservoirs. Most of the favorable bands have been through wash washing at medium-intensive levels, while the conventional untabulated samples with permeability below  $50 \times 10^{-3} \mu\text{m}^2$  are mostly free of water washing. Therefore, it is suggested that the presence of favorable bands in the untabulated reservoirs is a major factor impacting the hydrocarbon recovery of untabulated sands.

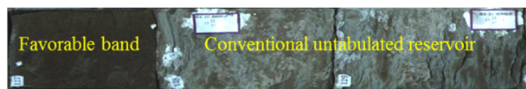


Figure 1. Core characteristics of untabulated reservoirs

Table 1. Permeability statistics of the five coring wells with high coring density

Type	Permeability Range ( $\times 10^{-3} \mu\text{m}^2$ )			
	1-10	10-50	50-500	>500
Sample proportion (%)	44.8	25.7	25.7	3.7
Layer proportion (%)	36.2	24.8	32.6	6.4

### 2.2 Micro pore structure characteristics of untabulated reservoirs

Comparison of the mercury intrusion curves of the favorable bands and conventional untabulated reservoirs (Fig. 2) shows that the conventional untabulated reservoir is found with a lower maximum mercury injection saturation, lower residual mercury saturation, higher mercury withdrawal efficiency, and preferred median-saturation pressure. In other words, the conventional untabulated reservoir, compared with the favorable band, has smaller pore-throat radii and higher displacement pressure.

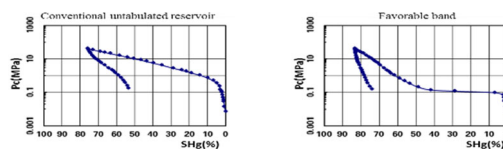


Figure 2. Comparison of the mercury intrusion curves of the conventional untabulated reservoir and favorable band

11 samples of the on-sheet and untabulated reservoirs in the X oilfield are put through the constant-rate mercury intrusion tests (specifically, 3 for the tabulated reservoir (in other words, included in the reserve sheet), 4 for the favorable band, and 4 for the conventional untabulated reservoir), which implies considerable differences of throat radii of the different samples (Fig. 3). In terms of the samples of the tabulated reservoir, the throat radius range is expanded and the proportion of larger throats is higher, with the radius peak generally occurring above  $7 \mu\text{m}$ . For the favorable band, the throat radius distribution is closer to that of the on-sheet reservoir, with the radius distribution peak occurring in  $5-7 \mu\text{m}$ . At last, the conventional untabulated reservoir is found with a narrow range of the throat radius, with the peak generally below  $5 \mu\text{m}$ .

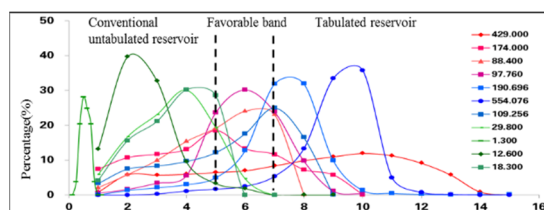


Figure 3. Throat radius distribution of core samples with varied permeability

### 3. Deposition mechanisms of untabulated reservoirs

#### 3.1 Sedimentary models of varied types of sands

The formation and distribution of untabulated reservoirs are controlled by the original sedimentary environment and associated conditions. The deltaic distributary plain facies mainly develops the (fluvial) channel sand, with sufficient clast supply. The occurring of the untabulated reservoir is mostly attributed to breach and overbank floods. Due to the high-energy sedimentary environment, the untabulated reservoir typically contains multiple medium-high permeability banded sands. Moreover, the untabulated sand body is seen with rapid lateral thinning and, because of the quick horizontal decline of the sedimentary environment energy and a lack of clastic supplement. The outward extension of the inter-channel sand body from the channel is short. Hence, in a planar view, the medium-high permeability untabulated sand presents itself as a sand body attached to the effective (on-sheet) sand body in the forms of edging and bridging. The coring well data shows that the farthest extension of medium-high permeability sand from the effective sand is only 25 m, which is rather difficult to identify in the case of the current well pattern.

The inner front of the delta is subjected to the joint effects of the river and lake and typically develops large-area sheet sands. The lake is found with high lateral continuity of energy. Therefore, the massive coarse-grained clasts, entrained and supplied by the river, deposit with decreasing thickness outward from the two river banks, with the degrading lake energy, which results in the successive formation of the fluvial channel sand, sheet sand, and medium-high permeability untabulated sand. As for the fine-grained clasts, the corresponding sediments reach farther, with the help of waves, and the connected low-ultra low permeability untabulated sands are formed. In the deltaic inner front sedimentary environment, the extension of the medium-high permeability sand is larger—the coring well data shows that the farthest extension of the medium-high permeability sand from the effective sand is 200 m.

The outer front facies is mainly affected by the lake. In such a low-energy environment lacking clastic supply, the untabulated reservoir mainly presents itself as the low and ultra-low permeability sand. The development area and probability of medium-high permeability sands are higher in the outer front I zone than in the outer front II zone. The untabulated reservoir in the latter is found with a predominance of connected low and ultra-low permeability sands and sporadic isolated medium-high permeability sands (Fig. 4).

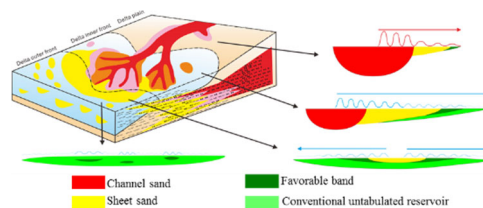


Figure 4. Sedimentary models for different sedimentary environments

#### 3.2 Planar distribution characteristics of untabulated reservoir sands

According to the planar development location of untabulated sands and the planar sedimentary facies distribution, 5 planar development types of untabulated reservoirs are identified, namely the edging type (bridging with the channel sand), the embedding type (embedded into the main and non-main sands), the extending type (that is no less than 200 m away from the effective sand), the connected type (connected untabulated sands), and the isolated type (untabulated sands scattered in mudstone).

Analysis of the corresponding untabulated sand types of the collected samples shows that the development proportion of the favorable band is the highest in the edging-bridging type of the underwater distributary fluvial channel sand and reaches 88%, associated with only the conventional untabulated reservoir accounting for only 12%. The development proportion of the favorable band in the untabulated sand embedded into the main or non-main thin sands reaches 87%, with the corresponding proportion of the conventional untabulated reservoir of 13%, similar to the case of the edging-bridging type. The favorable band proportion is 75% in the extending type, with the conventional untabulated sand proportion of 25%. The least proportion of the favorable band is found in the connected type (only 15%), with the corresponding conventional untabulated sand reservoir proportion reaching 85%. In summary, the development probability of favorable bands ranks from high to low as the edging type, embedded type, extending type, and the connected type.

The water absorption statistics show that for the above four planar types of untabulated sands, the water absorption ratios of favorable bands rank as the edging type, embedded type, extending type, and connected type, which is consistent with the development probability regularity of favorable bands. The concentrated zone of favorable bands in the untabulated reservoir has higher produced degrees. Therefore, the favorable band is vital for further potential tapping of the remaining oil.

The sedimentary environments and planar distribution locations of conventional untabulated reservoirs and favorable bands (both of the untabulated reservoir) are clarified via investigation of the sedimentary patterns and planar distribution characteristics of untabulated reservoirs. The favorable band mainly occurs in the distal sedimentary environment of the delta inner front and the proximal sedimentary environment of the delta outer front. The sands of the favorable band favorably contact with the

fluvial channel sand, and main and non-main thin sands. As for the conventional untabulated reservoir, it mainly occurs in the distal zone of the outer front, and some in the medium zone of the outer front. The conventional untabulated reservoir is dominated by the lake and typically occurs as a connected areal development or contacting with the mudstone.

#### 4. Production characteristics of untabulated reservoirs

To clarify the production behaviors of the untabulated reservoir sands of various types with varied injection-production modes, five physical model simulation experiments and numerical simulations are performed for the various types of untabulated sands. Sample #1 is designed to simulate the separate recovery of the conventional untabulated reservoir. Sample #2, for the parallel recovery of the favorable band and conventional untabulated reservoir; Sample #3, for the parallel recovery of the favorable band and conventional untabulated reservoir, with only the latter perforated; Sample #4, for the cascade recovery of the favorable band and conventional untabulated reservoir; Sample #5, for the recovery of the pinch-out favorable band. The experimental preparation and sample treatment (mainly including the drying, vacuuming, oil and water saturation, parameter calculation, and finally water flooding test) are done in accordance with the Chinese national standard SY/T 5358-2002.

##### 4.1 Results of the physical model and numerical simulations

The total recovery factors of the five physical models (five recovery approaches) are all above 40%, and yet the recovery of Samples #2 and #3 are associated with considerable production interference harmful to the effective exploitation of the conventional untabulated reservoir. The recovery approaches of Samples #4 and #5 are found in favor of producing from the conventional untabulated reservoir.

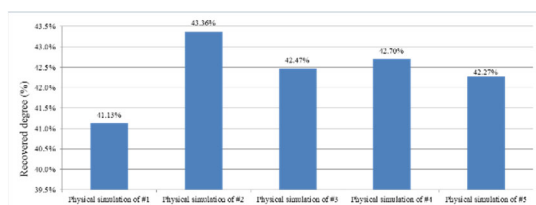


Figure 5. Histograms of recovery factors of the physical models

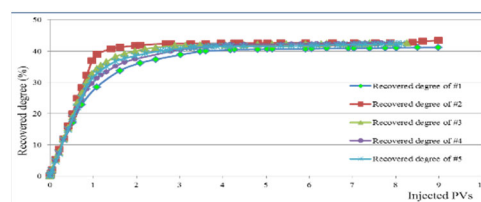


Figure 6. Comparison of the recovered degrees of the physical models

The numerical simulation (Figs. 7 and 8) demonstrates that the highest recovery factor is attributed to the parallel recovery of the favorable band and conventional untabulated reservoir (Sample #2) and reaches 43.25%; however, this recovery approach suffers from intensive interlayer interference, which leads to the limited recovery of the conventional untabulated reservoir (with the contributions of only 23.8% to the total). Moreover, the least recovery of the conventional untabulated reservoir with the contributions of only 17.8% is associated with the recovery approach of Sample #3, in which the flow rate and streamline indicate occurring of cross flow and the production is mainly supplied by the non-perforated favorable band (the recovered degrees of the conventional untabulated reservoir are low). The recovery approaches of Samples #4 and #5 are in favor of production stimulation of the conventional untabulated reservoir. The recovery factors of the cascade recovery for the physical and numerical simulation reach 42.7% and 42.10%, respectively. The corresponding flow rate and streamline demonstrate that these two approaches help to promote the recovery of the conventional untabulated reservoir.

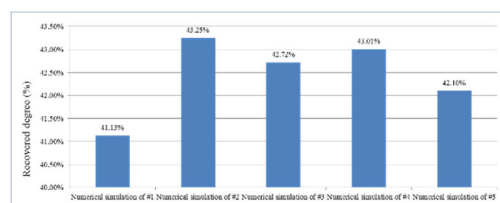


Figure 7. Histograms of recovery factors of the numerical simulation

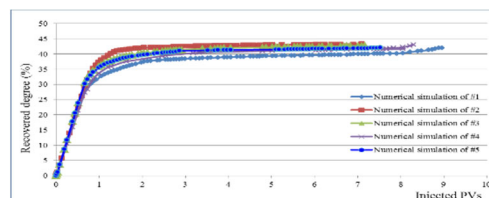


Figure 8. Comparison of recovered degrees of numerical simulation

The physical and numerical simulations demonstrate that the separate recovery of the conventional untabulated reservoir can present the total recovery factor above 40%, with the slow growth of water cut, and the production of the conventional untabulated reservoir is highly disturbed



by the favorable band. In the untabulated reservoir containing the favorable band, the injected water always finds the dominant channel via the favorable band, regardless of whether the favorable band is perforated or not. Under such circumstances, it is difficult to exploit the conventional untabulated reservoir. In the cascade arrangement of the favorable band and conventional untabulated reservoir, the recovery performance of the evenly-displaced favorable band side is better, and yet the contributions of the conventional untabulated reservoir are lower than the injection of the conventional untabulated reservoir. It should be noted that in the case of either the cascade arrangement or parallel arrangement of sands, the simultaneous recovery of the favorable band and conventional untabulated reservoir, the contributions of the favorable band always exceed 60%, which make it the main contributor in the untabulated reservoir.

#### 4.2 Numerical simulation of the production interference in parallel recovery

To determine whether or not the joint recovery of the favorable band and the conventional untabulated reservoir is associated with interference, and if any, how strong it may be, a parallel recovery experiment is designed to calculate the separate contributions of the two types of untabulated reservoirs. The samples of the favorable band and conventional untabulated reservoir are separately put into different core holders and then flooded in a parallel arrangement. The liquid, oil, and water production are measured in the outlets also in a separate fashion to compute the respective contributions to the total liquid and oil production.

The model parameters for the production interference simulation of the parallel recovery are listed below (Fig. 9). The model parameters are  $4.5 \times 4.5 \times 30$  cm (for each core sample), with the porosity of 18%–23%, the permeability of 17.8–80 mD, the pore volume of 182.25 cm<sup>3</sup>, oil initially in place 100.23 cm<sup>3</sup>, and the initial oil saturation of 55%. The injection rate during flooding is 2 mL/min.

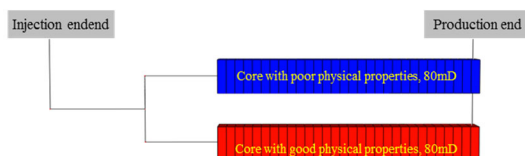


Figure 9. Schematic diagram of the parallel recovery

The simulation ends, as the water cut reaches 98%. By the end of the simulation, the ultimate recovery factor is 41.12%. As shown by the recovered degree versus injected water (expressed as multiples of pore volumes, injected PV), When the injection volume is from 0 to 1 PV, it is the rapid growth of the recovered degrees. From 1 PV to 3 PV, the recovered degree climbs up steadily. After 3 PV, the injection is low-efficient or ineffective. The favorable band presents considerable interference. After the water-free production, the flow rate of the favorable band is far higher than that of the conventional untabulated reservoir. The produced oil is mainly from the

favorable band (contributing 87.5%; Figs. 10 and 11). This result is similar to those of numerical simulations of Samples #3 and #2, which demonstrates that the joint recovery in such reservoirs is unfavorable for the exploitation of the conventional untabulated reservoir.

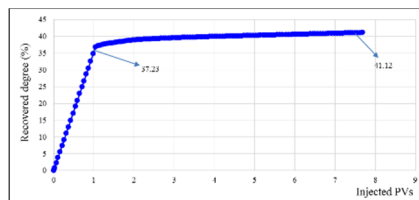


Figure 10. Recovered degrees of numerical simulation

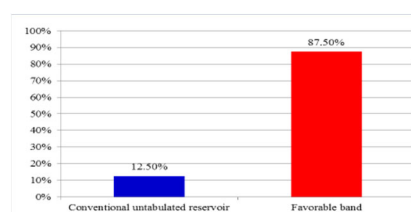


Figure 11. Contributions of the conventional untabulated reservoir and favorable band

The conventional untabulated reservoir is severely impacted by the favorable band. The actual production is much more complex than the simulated one and therefore it is safe to say that it is highly difficult to effectively recover the conventional untabulated reservoir in the case of joint recovery. In theory, the cascade recovery of the conventional untabulated reservoir and favorable band in which the injection well is placed in the untabulated reservoir is expected with better recovery performance. Nonetheless, the actual production suffers from severe interlayer interference and it is impossible to build the separate well pattern for recovery. Hence, it is recommended that the development of the untabulated reservoir should preferably recover the un-produced favorable band.

## 5. Conclusions

Under the guidance of the above findings, the type-specific adjustment of the untabulated sands (that are not included in the reserve sheet) of the D well district is implemented. For the favorable band with permeability above  $50 \times 10^{-3} \mu\text{m}^2$ , the adjustment combines the injection rate enhancing and control. For the highly-permeable layer of the favorable band that is already producing, the ineffective injection is controlled after testing and adjustment. For the non-producing favorable band with remaining oil potential, the refined layer division is performed for recovery. Moreover, for the low-permeability untabulated sand with the permeability of  $(10-50) \times 10^{-3} \mu\text{m}^2$ , the injection-production adjustment is optimized to improve the pressure gradient. At last, for the ultra-low permeability untabulated sand with permeability below  $10 \times 10^{-3} \mu\text{m}^2$ , an attempt is made for

the precise-control fracturing that highlights targeted reservoir stimulation. The adjustment of the D well district results in effective control of water injection and liquid production and the adjustment performance is considerable, considering the cumulative oil gain of 1286000 tons. The development adjustment performance of the D well district validates the identified deposition mechanisms and production characteristics of the various untabulated reservoir sands.

(1) The untabulated reservoir presents high heterogeneity. A considerable discrepancy is found between the micro-pore structures of the conventional untabulated reservoir and favorable band. The physical properties and pore-throat characteristics of the favorable band, compared with those of the conventional untabulated reservoir, are closer to those of effective sands of the tabulated reservoir (included in the submitted reserve sheet).

(2) The deltaic distributary plain facies is highly subjected to the high-energy river and the resultant untabulated reservoir largely contains favorable bands. Due to the joint effects of the river and lake, in the delta inner front facies, the clastic sediments gradually thin outward from both sides, and the favorable band mainly develops within 200 m from the effective sand. As for the conventional untabulated reservoir, it can reach farther away, with the help of waves, and deposit in a connected pattern. Affected by the lake, the medium zone of the outer delta front representing a low energy environment is seen with the predominance of the conventional untabulated reservoir, and the favorable band is found with limited development in the proximal zone of the outer delta front.

(3) In a planar view five types of untabulated reservoir sands are identified, namely, the edging, embedded, extending, connected, and isolated types. The favorable band mostly occurs as the edging, embedded, and extending types, while the conventional untabulated reservoir generally presents stable connected areal development and is mainly of the connected and isolated types.

(4) The favorable band severely interferes with the production of the conventional untabulated reservoir and highly impacts the recovered degree of the latter. The contributions of the favorable band to production are much higher than those of the conventional untabulated reservoir. In other words, the favorable band is the main producer of the untabulated reservoir.

## Acknowledgements

Funded by the 13<sup>th</sup> Five-Year-Plan National Science and Technology Major Project “Development of Large Oil and Gas Fields and Coalbed Methane—The Demonstration Area of the Water Flooding Water Controlling and Efficiency Enhancement of the Eastern Xing-6 District” (Grant No. 2016ZX05054-002)

## References

1. Xu Chaopeng. Method Of Enhancing The Developed Degree Of The Untabulated Reservoirs. *Petroleum*

- Geology and Oilfield Development in Daqing* 33(4):57-61(2014)
2. Liu Ding-ceng, Wang Qi-min, Li Bo-hu. Development of multi-sandstone reservoirs in Daqing oil field. *Petroleum Industry Press*(1996).
3. Gao Da-peng, Ye Ji-gen, Hu Yong-le, et al. An evaluation model for stratified water injection in multilayer reservoirs. *Petroleum Exploration and Development* 42( 6), 711-715(2015).
4. Fu Guang-qun, Wei Ze-gang, Guo Hong-wei, et al. Characteristics and recovery method of untabulated reservoirs in Xingnan oilfield. *Journal of Daqing Petroleum Institute* 27(4), 15-17(2003).
5. Liu Yi-kun, Wang Feng-jiao, Hu Chao-yang, et al. Study on oil / water percolation in thin and poor pay zone. *Special Oil and Gas Reservoirs* 20( 5), 98-101(2013).
6. Gao Da-peng, Ye Ji-gen, Li Qi, et al. An independent development method of low permeability oil thin layers with extreme high water cut in Changyuan Structure, Daqing oilfield. *Oil and Gas Geology* 38(1), 181-188(2017).
7. Zhang Dong, Di Jjing-dong, Li Jie, et al. Effective development technology of unbooked reservoirs in Daqing La-Sa-Xing oilfield. *Petroleum Geology and Oilfield Development in Daqing* 28(5), 112-118(2009).
8. Qi Chun-yan. Adjustments on thin and poor reservoir and unworkable reserves in La-Sa-Xing oilfield. *Petroleum Geology and Oilfield Development in Daqing* 29(2), 64-69(2010).
9. Xu Xiao-ping. Micro-pore structures of the untabulated reservoir and the characteristics of polymer injection. *Petroleum Geology and Oilfield Development in Daqing* 31(4), 135-138( 2012).
10. Xu Pengchao. Method of enhancing the developed degree of the untabulated reservoirs. *Petroleum Geology and Oilfield Development in Daqing* 33(4), 57-61( 2014).
11. Cui Yue, Shi Jingping. Experiment on the seepage features for the untabulated reservoirs in Daqing oilfield. *Petroleum Geology and Oilfield Development in Daqing* 36(2), 69-72(2017).
12. Mechanism of CO<sub>2</sub> enhanced oil recovery in shale reservoirs[J]. Hai-Bo Li, Zheng-Ming Yang, Rui-Shan Li, Ti-Yao Zhou, He-Kun Guo, Xue-Wei Liu, Yi-Xin Dai, Zhen-Guo Hu, Huan Meng. *Petroleum Science*. 2021(06)
13. Jin-you DAI, Jing YAO, Meng KONG, Jing WANG. New Method to Quantitatively Describe Remaining Oil by Dynamic Data[A]. *Proceedings of 2016 International Conference on Electrical Engineering and Automation (ICEEA2016)* [C]. 2016
14. Yu Qi-tai. A Study On Remaining oil[J]. *Petroleum Exploration and Development*, 1997, 24(2):46-50
15. Quick assessment to ascertain technical rational well spacing density in artificial water flooding oilfield[J]. Hu Gang, Tian Xuanhua, Liu Quanwen, Yi Linzi, Liu

- Dawei, Li Pengchun. *Journal of Petroleum Science and Engineering* . 2021
16. The study on exploitation potential of original low-oil-saturation reservoirs[J] .Sun Yingying, Zhang Shanyan, Wei Xiaofang, Sang Guoqiang, Minghui Zhou, Huang Jia, Yang Jiru. *Petroleum Research* . 2020 (1)
  17. Effect of displacement rates on fluid distributions and dynamics during water flooding in tight oil sandstone cores from nuclear magnetic resonance (NMR) [J] . Meng Chen, Jiakai Dai, Xiangjun Liu, Yan Kuang, Zhongtao Wang, Shunchao Gou, Minjun Qin, Min Li. *Journal of Petroleum Science and Engineering* . 2020 (C)
  18. Research the Electromagnetic Detecting Electrical Parameters Through the Casing[A]. *Proceedings of IEEE 2011 10th International Conference on Electronic Measurement & Instruments (ICEMI'2011) VOL.04[C]*. 2011
  19. Simulation of Residual Oil Distribution Based on 2D-network Model[A]. *2010 Information and Management Sciences--Processing of the Ninth International Conference on Information and Management Sciences[C]*. 2010
  20. Sedimentary characteristics and pattern of distributary channels in shallow water deltaic red bed succession: A case from the Late Cretaceous Yaojia formation, southern Songliao Basin, NE China[J] . Li Zhang, Zhidong Bao, Luxing Dou, Dongsheng Zang, Shuwei Mao, Jian Song, Jiahong Zhao, Zecheng Wang. *Journal of Petroleum Science and Engineering* . 2018
  21. Fluvialite fining-upwards cycles and the magnitude of palaeochannels[J] . M. R. Leeder. *Geological Magazine* . 1973 (3)
  22. Modeling of CO<sub>2</sub> solubility in crude oil during carbon dioxide enhanced oil recovery using gene expression programming[J] . Alireza Rostami, Milad Arabloo, Arash Kamari, Amir H. Mohammadi. *Fuel* . 2017
  23. Capillary driven flow in nanochannels – Application to heavy oil rheology studies[J] . Saeed Mozaffari, Plamen Tchoukov, Ali Mozaffari, Jesus Atias, Jan Czarnecki, Neda Nazemifard. *Colloids and Surfaces A: Physicochemical and Engi* . 2017
  24. Relationship between bulk foam stability, surfactant formulation and oil displacement efficiency in porous media[J] . Kofi Osei-Bonsu, Paul Grassia, Nima Shokri. *Fuel* . 2017
  25. Numerical simulations of seepage flow in rough single rock fractures[J]. Qingang Zhang, Yang Ju, Wenbo Gong, Liang Zhang, Huafei Sun. *Petroleum* . 2015
  26. Impact of pore-scale three-phase flow for arbitrary wettability on reservoir-scale oil recovery[J] . Adnan Al-Dhahli, Sebastian Geiger, Marinus I.J. van Dijke. *Journal of Petroleum Science and Engineering* . 2014
  27. A New Method base on Water Drive Curve for Determining the Reasonable Injection-Production Ratio for High Water-Cut Oilfield[J]. ZHANG Zhang, QUAN Honghui, XU Zhongbo, HE Xinrong, LI Jun. *Acta Geologica Sinica (English Edition)* . 2015(S1)
  28. Calculation on a reasonable production/injection well ratio in waterflooding oilfields[J] . Cunyou Zou, Yuwen Chang, Guohui Wang, Lifeng Lan. *Petroleum Exploration and Development Online* . 2011(2)
  29. Cui Yue. Experiment on the seepage features for the Untabulated Reservoirs in Daqing Oilfield. *Petroleum Geology and Oilfield Development in Daqing*36(02),69-72(2017)
  30. Xiao Lu-chuan, Cao Wei-fu , Xu Yun-ling. Characteristics of non-Darcy flow velocity of oil-water phases in extra-low permeability reservoirs. *Petroleum Geology and Oilfield Development in Daqing*26(5),61-63(2007)